Inhibition Effect of Deanol on Mild Steel Corrosion in Dilute Sulphuric Acid

Roland Tolulope Loto[a,b,*], Cleophas Akintoye Loto[a,b] and Abimbola Patricia Popoola[b]

[a]*Department of Mechanical Engineering, Covenant University, Ota, Ogun State, Nigeria.*

[b]*Department of Chemical, Metallurgical and Materials Engineering, Tshwane University of Technology, Pretoria, South Africa.*

ABSTRACT

The influence of deanol on the corrosion behaviour of mild steel in dilute sulphuric acid with sodium chloride addition was studied by means of mass-loss, potentiodynamic polarization, electrode potential monitoring, scanning electron microscopy and statistical analysis. Results show that deanol performed excellently with a maximum inhibition efficiency of 97.9 % obtained from the mass loss technique and 98.23 % from the potentiodynamic polarization tests at the maximum deanol concentration evaluated. Polarization studies show that the amino alcohol is a cathodic type inhibitor. Adsorption of deanol on the steel surface was observed to obey the Langmuir and Frumkin adsorption isotherms. Scanning electron microscopy studies confirmed the corrosion protection property of deanol to be through adsorption on the mild steel surface while statistical evaluation showed the overwhelming influence and significance of inhibitor concentration on inhibition efficiency compared with exposure time.

1. Introduction

Mild steel has excellent mechanical properties. Its low cost allows for extensive use as the material of construction in petroleum industries, chemical processing plants, marine applications, boilers, refinery plants, extractive industries, etc. However, its application under these industrial conditions subjects it to rapid corrosion attack especially in applications involving the extensive use of sulfuric acid and other corrosive media due to their wide range of applications, including domestic acidic drain cleaner, electrolyte in lead-acid batteries and various cleaning agents.[1] The most cost-effective and practical corrosion control technique for effectively preventing the occurrence or reducing the severity of corrosion is to alter the electrochemical nature of the environment with chemical compounds known as inhibitors.[2,3] Effective corrosion inhibition is subject to the chemical composition, molecular structure and affinity of the inhibiting compound with the metallic alloy surface. Deanol has been used for corrosion prevention in concrete with mixed results.[4–7] The compound adsorbs through concrete resulting in the formation of a complex precipitate of protective film, which adsorbs onto the metal surface. This provides an impenetrable barrier to metal dissolution that acts to stifle cathodic and or anodic electrochemical corrosion reactions taking place at the metal/solution interface. This investigation aims to evaluate the corrosion inhibition properties of deanol on the electrochemical behaviour of mild steel in aqueous dilute sulphuric acid at ambient temperature of 25 °C.

2. Experimental

2.1. Materials

The mild steel sample for this research was obtained in the open market and analyzed at the Applied Microscopy and Tribo-electrochemical Research Laboratory, Department of Chemical and Metallurgical Engineering, Tshwane University of Technology, South Africa. The mild steel has the nominal percentage composition: 0.401 C, 0.169 Si, 0.440 Mn, 0.005 P, 0.012 S, 0.080 Cu, 0.008 Ni, 0.025 Al, and the rest are Fe.

2.2. Inhibitor

Deanol (MDMAE) is a colourless, transparent liquid and was used as an inhibitor. The chemical structure of MDMAE is shown in Fig. 1. It consists of a nitrogen atom chemically attached to a hydroxyl group. The *molecular formula* is $C_4 H_{11} NO$, while the molar mass is 89.14 g mol^{-1}. MDMAE was prepared in volume concentrations of 2.5 %, 5 %, 7.5 %, 10 %, 12.5 % and 15 % per 200 mL of acid solution each.

2.3. Test Media

A solution of 0.5 M tetraoxosulphate (VI) acid with 3.5 % recrystallized sodium chloride (Analar grade) was prepared with distilled water and was used as the corrosion test media.

2.4. Preparation of Test Specimens

A cylindrical mild steel rod with a diameter of 14.5 mm was carefully machined and cut into a number of test specimens of average dimensions in lengths of 6 mm. A 3 mm hole was drilled at the centre for suspension. The steel specimens were then thoroughly rinsed with distilled water and cleansed with acetone for mass loss analysis. The linear polarization technique involved grinding the two surface ends of each specimen with silicon carbide abrasive papers of 80, 120, 220, 800 and 1000 grit before being polished with 6 μm to 1.0 μm diamond paste, washed with distilled water, rinsed with acetone, dried and stored in a desiccator before the test.
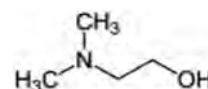

Figure 1 Chemical structure of deanol (MDMAE).[8–9]

* To whom correspondence should be addressed. E-mail: tolu.loto@gmail.com

2.5. Mass-loss Experiments

Weighed test species were fully and separately immersed in 200 mL of the test media at specific concentrations of the MDMAE for 432 h at an ambient temperature of 25 °C. Each of the test specimens was taken out every 72 h, washed with distilled water, rinsed with acetone, dried and re-weighed.

The corrosion rate (R) was determined from Equation 1:[10]

$$R = \left[\frac{87.6W}{DAT} \right] \qquad (1)$$

where W is the mass loss in milligrams, D is the density in g cm^{-2}, A is the area in cm^2, and T is the time of exposure in hours. The % IE was calculated from the relationship in Equation 2.[11]

$$IE\% = \left[\frac{R_1 - R_2}{R_1} \right] \times 100 \qquad (2)$$

R_1 and R_2 are the corrosion rates in the absence and presence of predetermined concentrations of MDMAE. The % IE was calculated for all the inhibitors every 72 h during the course of the experiment, while the surface coverage was calculated from the relationship:[12]

$$\theta = \left[1 - \frac{W_2}{W_1} \right] \qquad (3)$$

where θ is the amount of adsorbate adsorbed per gram (or kg) of the adsorbent, and W_1 and W_2 are the mass loss of mild steel coupon in free and inhibited acid chloride solutions, respectively.

2.6. Open-Circuit Potential Measurements

A two-electrode electrochemical cell with a silver/silver chloride reference electrode was used. The measurements of circuit potential (OCP) were obtained with Autolab PGSTAT 30 ECO CHIMIE potentiostat. Resin-mounted test electrodes/specimens with an exposed surface of 165 mm^2 were fully and separately immersed in 200 mL of the test media (acid chloride) at specific concentrations of MDMAE for a total of 288 h. The potential of each of the test electrodes was measured every 48 h.

2.7. Linear Polarization Resistance

Linear polarization measurements were carried out by using a cylindrical coupon embedded in resin plastic mounts with an exposed surface of 165 mm^2. The electrode was polished with different grades of silicon carbide paper, polished to 6 μm, rinsed with distilled water and dried with acetone. The studies were performed at ambient temperature with an Autolab PGSTAT 30 ECO CHIMIE potentiostat and an electrode cell containing 200 mL of electrolyte, with and without the inhibitor. A graphite rod was used as the auxiliary electrode and a silver/silver chloride electrode (SCE) was used as the reference electrode. The steady-state open OCP was noted. The potentiodynamic measurements were then made from –1.5 V *versus* OCP to +1.5 V *versus* OCP at a scan rate of 0.00166 V s^{-1} and the corrosion currents were registered. The corrosion current density (j_{corr}) and corrosion potential (E_{corr}) were determined from the Tafel plots of potential *versus* log I. The corrosion rate (R), the degree of surface coverage (θ) and the percentage inhibition efficiency (% IE) were calculated as follows:

$$R = \frac{0.00327 \times j_{corr} \times E_q}{D} \qquad (4)$$

where j_{corr} is the current density in μA cm^{-2}, D is the density in g cm^{-3} and E_q is the specimen equivalent weight in grams.

The percentage inhibition efficiency (% IE) was calculated from the corrosion current density values by using Equation 2.

2.8. Scanning Electron Microscopy Characterization

The surface morphology of the uninhibited and inhibited mild steel specimens was investigated after mass-loss analysis in 0.5 M H$_2$SO$_4$ solutions by means of a Jeol scanning electron microscope (Jeol JSM – 7600F UHR Analytical FEG SEM) for which SEM micrographs were recorded.

2.9. Statistical Analysis

A two-factor single level ANOVA test (F-test)[13,14] was performed so as to investigate the significant effect of inhibitor concentration and exposure time on the inhibition efficiency values of MDMAE in the acid media.

3. Results and Discussion

3.1. Mass-loss Measurements

Mass-loss of mild steel at various time intervals, in the absence and presence of various MDMAE concentrations in 0.5 M H$_2$SO$_4$ acid at 25 °C was studied. The values of mass-loss (W), corrosion rate (R) and the percentage inhibition efficiency (% IE) are presented in Table 1. The decrease in corrosion rate corresponds with an increase in inhibitor concentration due to more inhibitor molecules being adsorbed on the metal surface. This results in a wider surface coverage on the steel surface. Figs 2, 3 and 4 show the variation of mass-loss, corrosion rate and percentage inhibition efficiency *versus* exposure time at specific MDMAE concentrations obtained from the values in Table 1. Observation of these figures shows the potency of MDMEA from three different perspectives of the mass loss analysis method, namely, the electrochemical influence of MDMAE in ameliorating the corrosive damage of the acid media. Fig. 5 depicts the variation of % IE with inhibitor concentration. The curves obtained show a progressive increase in % IE with increase in MDMAE concentration accompanied by a significant decrease in corrosion rate.

MDMAE forms a compact barrier film, which prevents the diffusion of Fe^{2+} to the liquid/metal interface, while at the same time it inhibits the diffusion of Cl$^-$/SO$_4^{2-}$ to the metal/liquid interface. The barrier becomes more protective as the number of MDMAE molecules increases, thus preventing dissolution of the steel specimens. The film is strongly adsorbed through physiochemical mechanisms wherewith it is chemically bonded onto the surface of the steel. Inspection of Table 1 shows MDMAE to be much more protective in 0.5 M H$_2$SO$_4$ at the early stages of exposure due to the abundance and exacerbating influence of chloride ions in NaCl. MDMAE cationic molecules are insufficient to effectively inhibit the migration of Cl$^-$/SO$_4^{2-}$ onto the steel[15,16] probably due to the low molecular size of Cl$^-$ ions that allows for easier diffusion. The inhibition efficiencies in both solutions are generally effective and give near similar results at higher concentrations of MDMAE.

Table 1 Data obtained from mass-loss measurements at 25 °C for mild steel in 0.5 M H$_2$SO$_4$ in presence of specific concentrations of MDMAE at 432 h (n = 1).

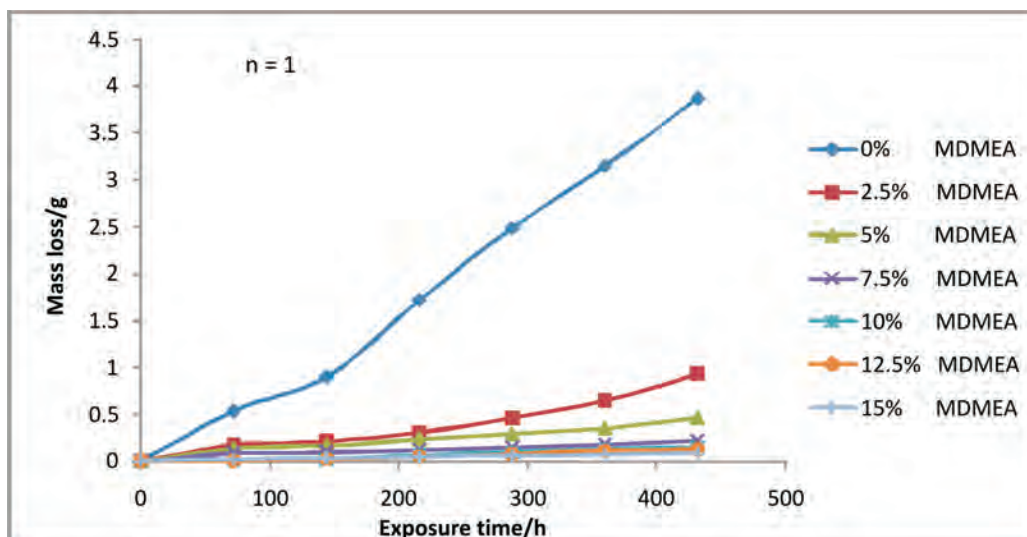| Sample	Inhibitor concentration/%	Mass loss/mg	Corrosion rate/mm y^{-1}	Inhibition efficiency/%
A	0	3.869	21.4712	0
B	2.5	0.932	4.2315	75.9
C	5	0.46	1.7607	88.1
D	7.5	0.213	0.894	94.5
E	10	0.141	0.6314	96.4
F	12.5	0.123	0.4822	96.8
G	15	0.08	0.3565	97.9

Figure 2 Variation of mass-loss with exposure time for samples (A–G) in 0.5 M H_2SO_4.
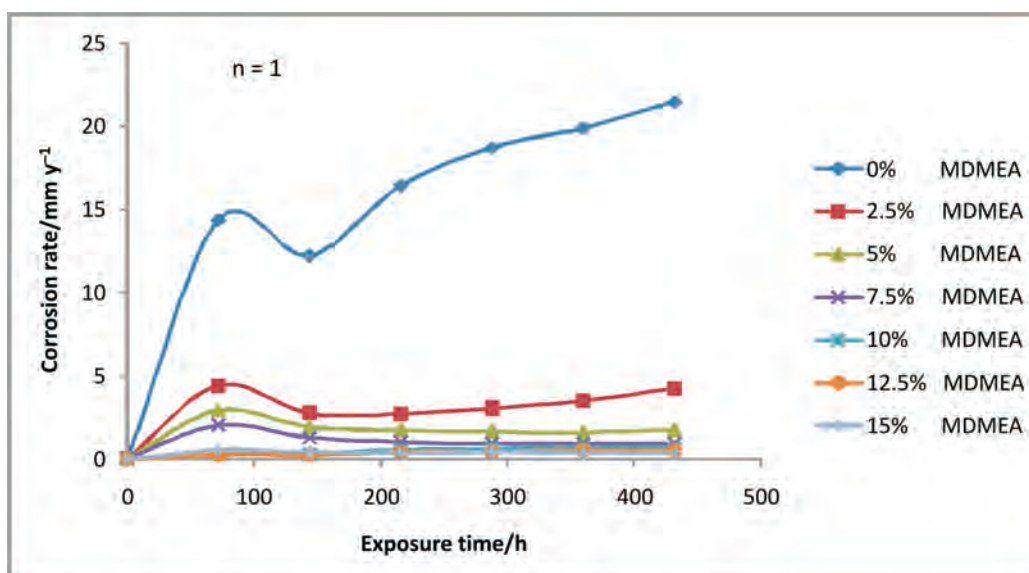

Figure 3 Effect of the concentration of MDMAE on the corrosion rate of mild steel in 0.5 M H_2SO_4.
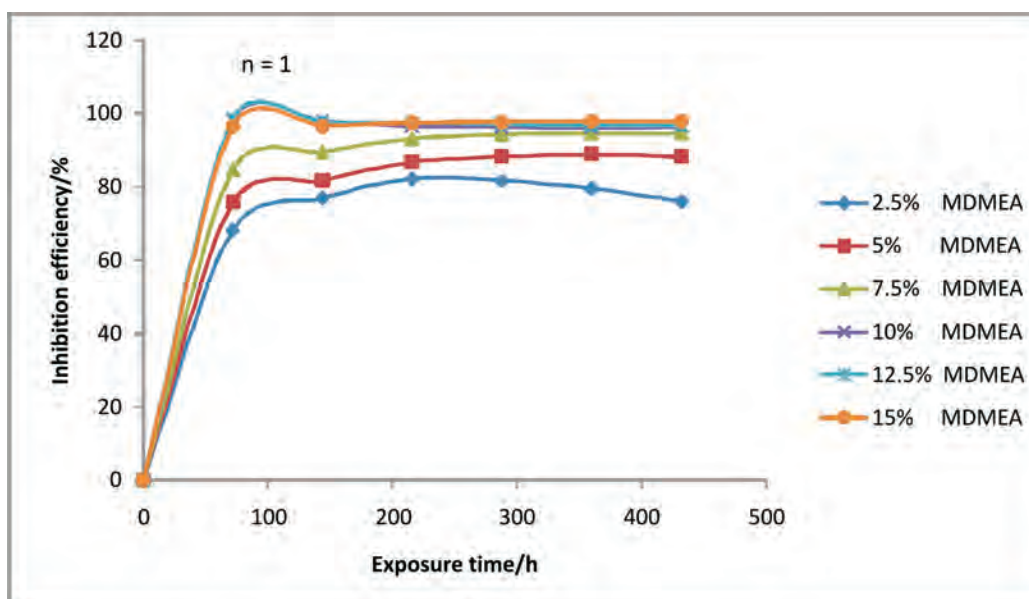

Figure 4 Plot of inhibition efficiencies of samples (A–G) in 0.5 M H_2SO_4 during the exposure period.

RESEARCH ARTICLE

R.T. Loto, C.A. Loto and A.P. Popoola,
S. Afr. J. Chem., 2015, **68**, 105–114,
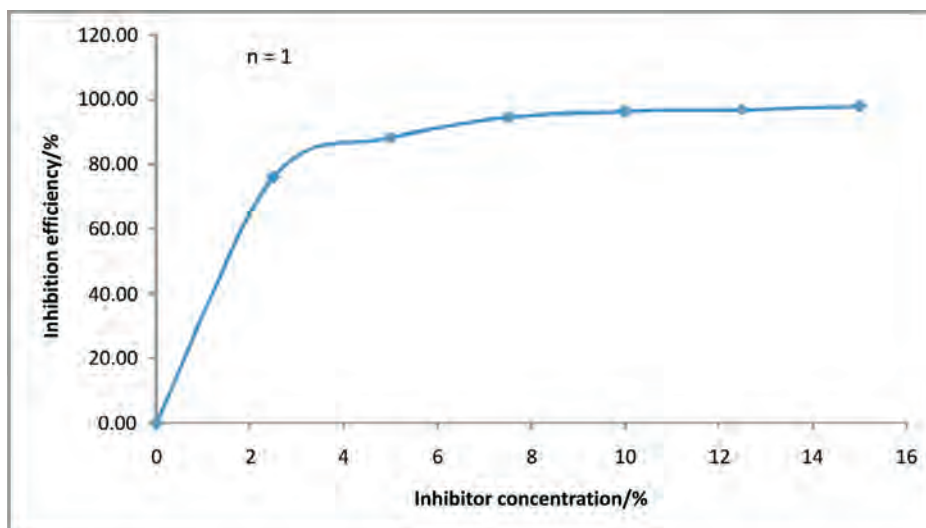<http://journals.sabinet.co.za/sajchem/>.

108

Figure 5 Variation of percentage inhibition efficiency of MDMAE with inhibitor concentration in 0.5 M H₂SO.

3.2. Open-Circuit Potential Measurement

The open-circuit potential value of the specimen electrodes was observed for a total of 288 h in the acid solution as shown in Table 2. Generally, a state of equilibrium was reached within 60 min. Fig. 6 shows the variation of open-circuit potentials with time in 0.5 M H_2SO_4 chloride solutions in the absence and presence of specific concentrations of MDMAE. A steady-state potential averaging ~300 mV was noticed in all MDMAE concentrations in the sulphuric acid chloride media. The control specimen (0 % MDMAE) reveals the corrosive nature of the sulphuric acid solution. The potential values progressed significantly towards more negative potentials; an indication that anodic dissolution is actively taking place in the absence of MDMAE, which results in specimen degradation and formation of corrosion products including oxides in solution. However, due to the influence of MDMAE in concentrations 2.5–15 %, the potential values shifted to positive potentials well below the potential at which corrosionoccurs. The corrosion risk is low due to the instantaneous action of the cationic species of the MDMAE ions, which inhibits the dissolution of the steel electrode through adsorption. This electrolytic mechanism blocks the active sites on the electrode and stifles the cathodic reaction.

The positive potential shift in the acid indicates the enhance-

Table 2 Data obtained from potential measurements for mild steel in 0.5 M H_2SO_4 in the presence of specific concentrations of MDMAE ($n = 1$).

Exp. time/h	MDMAE concentration/%						
	0	2.5	5	7.5	10	12.5	15
0	–477	–308	–311	–315	–319	–338	–327
48	–475	–310	–313	–318	–314	–320	–325
96	–514	–314	–310	–323	–318	–322	–314
144	–496	–311	–316	–319	–327	–317	–306
192	–498	–317	–314	–310	–322	–318	–291
240	–498	–309	–312	–304	–316	–312	–304
288	–516	–305	–309	–297	–311	–308	–299

ment of the steel's corrosion resistance in the presence of MDMAE, due to chemical adsorption (chemisorption) of the inhibitor cations onto the steel surface. The covalent bonding thatoccurs is responsible for the compaction barrier and strong adherence, which separates the steel from the corrosive species. This electrolytic action maintains the potential values in the domain of passivity.
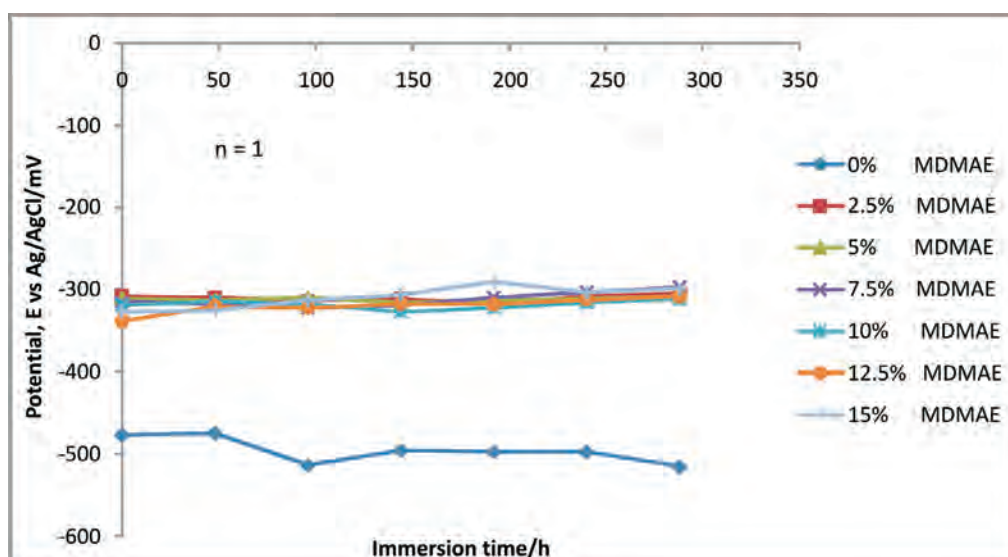

Figure 6 Variation of potential measurements with immersion time for MDMAE concentrations in 0.5 M H₂SO₄.

3.3. Polarization Studies

Potentiostatic potential was cursorily examined from –1.5 to +1.5 V *vs* Ag/AgCl at a scan rate of 0.00166 mV s^{-1}. The effect of the addition of MDMAE on the potentiodynamic plot of mild steel type 304 in 0.5 M H$_2$SO$_4$ solutions was studied at ambient temperature. Fig. 7 shows the polarization curves of the mild steel in the absence and presence of MDMAE at specific concentrations while Fig. 8 shows the relationship between % *IE* and inhibitor concentration for a polarization test in 0.5 M H$_2$SO$_4$. The effect of MDMAE corresponds with the value of its concentration in the acid solutions. As observed earlier from mass-loss analysis, the inhibition effect of MDMAE in 0.5 M H$_2$SO$_4$ is instantaneous due to the formation of a compact barrier film that prevents the diffusion of aggressive anions.

Results obtained from the linear polarization technique indicate that adsorbed MDMAE on the surface of the metal electrode retards the electrochemical process of corrosion. Anodic and cathodic currents were significantly influenced with increasing concentrations of MDMAE. Generally, the polarization scans exhibited almost similar behaviour (with a few exceptions) over the potential domain examined. The corrosion rate reduced drastically with differential changes in the electrochemical parameters. Thus, MDMAE significantly alters the electrochemical reactions responsible for corrosion. In addition, changes in the anodic Tafel constants in the presence of MDMAE signify that anodic dissolution reactions are slowed down by the surface blocking effect of the inhibitor. The cathodic Tafel constants show differing values due to the film-forming characteristics of MDMAE, which in effect suppresses hydrogen evolution reactions. The inhibitive action of the inhibitor is related to its adsorption and formation of a barrier film on the electrode surface.

The electrochemical variables, such as, corrosion potential (E_{corr}), corrosion current (i_{corr}), corrosion current density (j_{corr}), cathodic Tafel constant (*bc*), anodic Tafel slope (*ba*), surface coverage (*θ*) and percentage inhibition efficiency (% *IE*) were calculated and are given in Table 3. The corrosion current density (j_{corr}) and corrosion potential (E_{corr}) were established from the intersection of the extrapolated anodic and cathodic Tafel lines and % *IE* was calculated from Equation 2.

MDMAE showed anodic inhibiting tendencies in 0.5 M H$_2$SO$_4$ up till 5 % MDMAE concentration from the corrosion potential values (E_{corr}) in Table 3, probably due to the formation of the barrier film responsible for corrosion inhibition. This film prevents anodic dissolution due to the surface coverage and adsorption properties of the inhibitor. The inhibitor is first adsorbed onto the metal surface and hampers the passage of metal ions from the oxide-free metal surface into the solution, by merely blocking the reaction sites of the metal surface and thus affecting the anodic reaction mechanism. After 5 % MDMAE there is a progressive shift in the E_{corr} values till 15 % MDMAE to more negative potential, i.e. the direction of the potential shift is cathodic. The cathodic reaction is the reduction of water molecules on the steel surface. The adsorbed MDMAE molecules on the metal displace pre-adsorbed molecules within the metal/solution interface thereby obstructing their reaction. This in effect reduces the rate of hydrogen evolution and thus the cathodic reactions.

Classification of inhibitors on the basis of their influence on the electrochemical process is due to the displacement of the E_{corr}

Table 3 Data obtained from polarization resistance measurements for mild steel in 0.5 M H$_2$SO$_4$ in the presence of MDMAE (*n* = 1).

| Inhibitor Conc./%	Inhibitor conc./M	Corrosion rate/mm y^{-1}	Inhibition efficiency/%	Polarization resistance/Ω	E_{corr}/V	j_{corr}/A	j/A cm^{-2}	*bc*/V dec^{-1}	*ba*/V dec^{-1}
0	0	7.39	0	37.95	–0.453	1.05×10^{-3}	6.36×10^{-4}	0.133	0.297
2.5	0.000281	1.24	83.23	87.854	–0.389	1.76×10^{-4}	1.07×10^{-4}	0.042	0.234
5	0.000561	0.56	92.47	163.67	–0.382	7.91×10^{-5}	4.79×10^{-5}	0.035	0.213
7.5	0.000841	0.54	92.73	96.466	–0.461	7.63×10^{-5}	4.63×10^{-5}	0.090	0.021
10	0.001122	0.32	95.64	447.15	–0.795	4.58×10^{-5}	2.78×10^{-5}	0.068	0.157
12.5	0.001402	0.27	96.33	330.54	–0.555	3.85×10^{-5}	2.34×10^{-5}	0.070	0.050
15	0.001683	0.13	98.23	992.98	–0.822	1.85×10^{-5}	1.12×10^{-5}	0.138	0.061
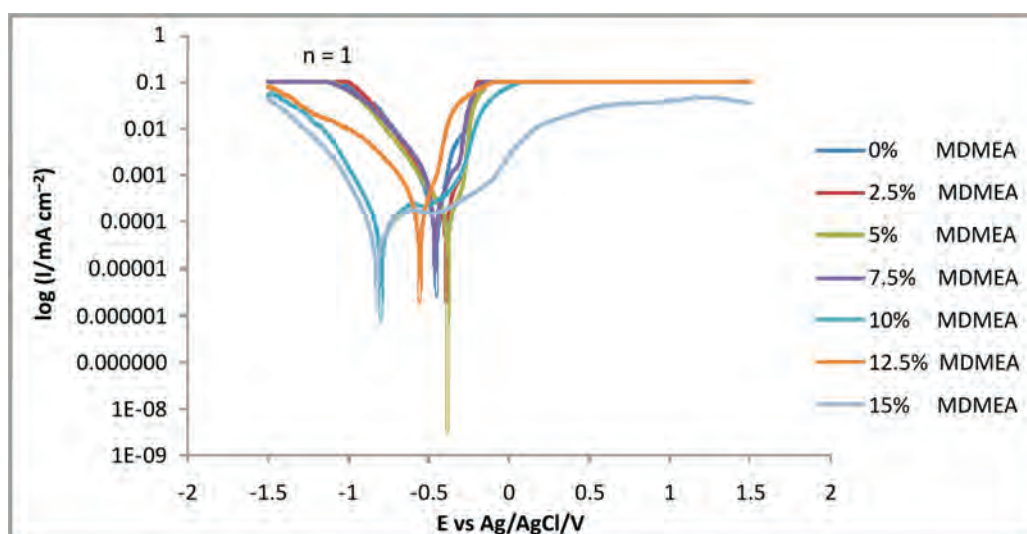
Figure 7 Comparison of cathodic and anodic polarization scans for low carbon steel in 0.5 M H$_2$SO$_4$ + 3.5 % NaCl solution in the absence and presence of specific concentrations of MDMAE.
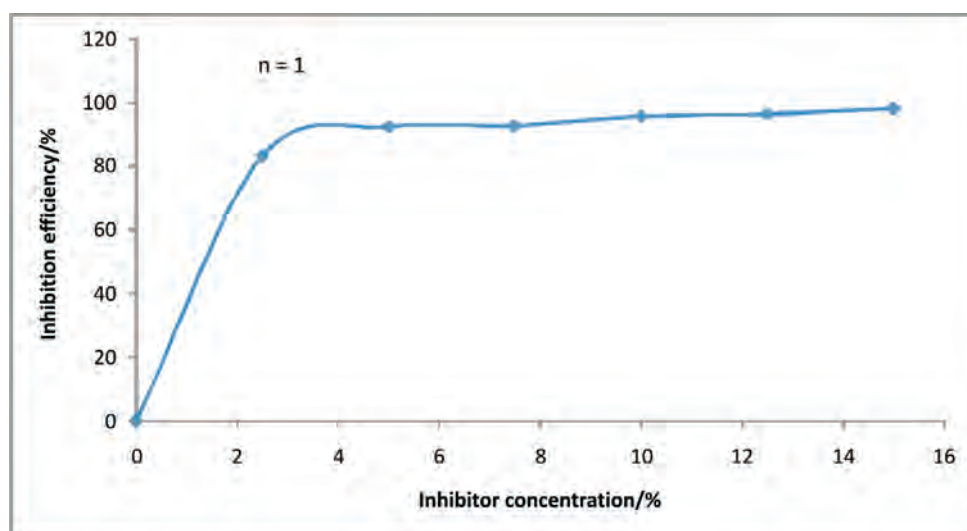
RESEARCH ARTICLE

R.T. Loto, C.A. Loto and A.P. Popoola,
S. Afr. J. Chem., 2015, **68**, 105–114,
<http://journals.sabinet.co.za/sajchem/>.

110

Figure 8 Relationship between % *IE* and inhibitor concentration for polarization test in 0.5 M H_2SO_4.

values. Displacement values greater than 85 mV in either direction show it is either an anodic or cathodic inhibitor. If displacement in E_{corr} is less than 85 mV, the inhibitor can be seen as mixed type. The maximum displacement of the E_{corr} value in H_2SO_4 in the anodic direction is –71 mV while in the cathodic direction its 369 mV, thus MDMAE is a cathodic-type inhibitor in the acid solutions. In Fig. 7 there is a significant displacement of potential values for 10 % and 12.5 % MDMAE concentration in H_2SO_4.

3.4. Mechanism of Inhibition

During the inhibition process, MDMAE molecules protonate in solution and become positively charged; the metal surface is also positively charged in the acid media. Cl^- and $SO_4{2-}$ ions are specifically adsorbed onto the metal and create an excess of negative charge on its surface.[17,18] This favours the adsorption of protonated MDMAE on the surface through electrostatic attraction and hence reduces the dissolution of Fe to Fe^{2+}. The values of inhibition efficiency and surface coverage suggest a chemisorption mechanism is responsible for covalent bonding in the adhesion process. Examination of the structure of MDMAE shows two potential sources of inhibitor-metal interaction. The unshared pair of electrons present on nitrogen within the amine functional group and the oxygen atom on the hydroxyl functional group is responsible for the characteristic reactions of MDMAE.

The amine nitrogen is sp^3 – hybridized and tetrahedral shaped. The nitrogen non-bonded electron pair acts like a substituent, the geometry is tetrahedral around nitrogen and the bond angles are all around 109 °. The sp^3 hybridized nitrogen is not rigid and can undergo rapid inversion. This attribute allows the molecular structure of MDMAE to form a compact film on the steel surface. This is chiefly responsible for the chemisorption mechanism with the steel through charge transfer between the polar species.[19–21]

The inhibition efficiency at lower concentrations in H_2SO_4 suggests the mechanism of formation of the inhibitor film is due to an initial increase of the anodic activity in some sites on the surface, probably the displacement of the first hydrated monolayers of the iron oxide formation. It is proposed that these anodic points can act as favourable anchorage points for the development of the inhibitor monolayer film. The presence of inhibitor causes a strong reduction of the anodic activity and helps in the formation of a protective layer on the surface that complex the chlorides ions, and thus reduces the threshold

Cl^-/OH^- ratio on the steel surface. After 5 % MDMAE/H_2SO_4 up to 15 % MDMAE/H_2SO_4 the E_{corr} displacement suggests cathodic inhibition.

The dominant cathodic process is the reduction of water molecules to produce H_2 gas according to the equation:

$$H_2O_{(surface)} + e^- \rightarrow h + OH^- \tag{5}$$

$$H + H_2O \rightarrow H_2 + OH^- \tag{6}$$

This process occurs simultaneously with the substitution process between the MDMAE in the aqueous solution and water molecules pre-adsorbed at the metal surface $[H_2O\ (ads)]^{22}$ as given in Equation 7:

$$MDMAE_{(sol)} + nH_2O_{(ads)} \rightarrow MDMAE^+_{(ads)} + nH_2O \tag{7}$$

where n represents the number of water molecules replaced by one molecule of MDMAE.

The inhibitor is adsorbed selectively on the metal due to the action of chloride ions. Accumulation of MDMAE allows for more readily available MDMAE cations to complex with the chloride ions. Adsorption occurs, accompanied by a change in potential difference between the metal and MDMEA inhibitor. This is a chemical adsorption process, which involves the donation of a pair of electrons present on the nitrogen atom to the iron metal.

3.5. Scanning Electron Microscopy

The SEM images of the low carbon steel surfaces before immersion in 0.5 M H_2SO_4 solution and after 432 h immersion with and without MDMAE additions are given in Fig. 9a–c, respectively. Fig. 9a shows the steel sample before immersion, the lined and jagged surfaces are due to cutting during preparation. Fig. 9b shows the steel surface after 432 h of immersion in 0.5 M H_2SO_4 without MDMAE, while Fig. 9c shows the steel surface in the acid medium with MDMAE. In the absence of MDMAE, a very rough and totally uneven surface is observed in Fig. 9b and a large number of macro pits and badly corroded topography of the mild steel coupons are visible as a result of the corrosive actions of chloride and sulphate ions[23,24] in Fig. 9b, indicating the actions of these ions in the facial corrosion of the steel. Their rapid transport and electrochemical activity due to their high electronegativity characteristics enhances the instantaneous rate of Fe^{2+} diffusion into the electrolyte. This causes the observed uniform and intergranular corrosion to occur with large macro pits. The morphology of the steel sample with MDMAE addition
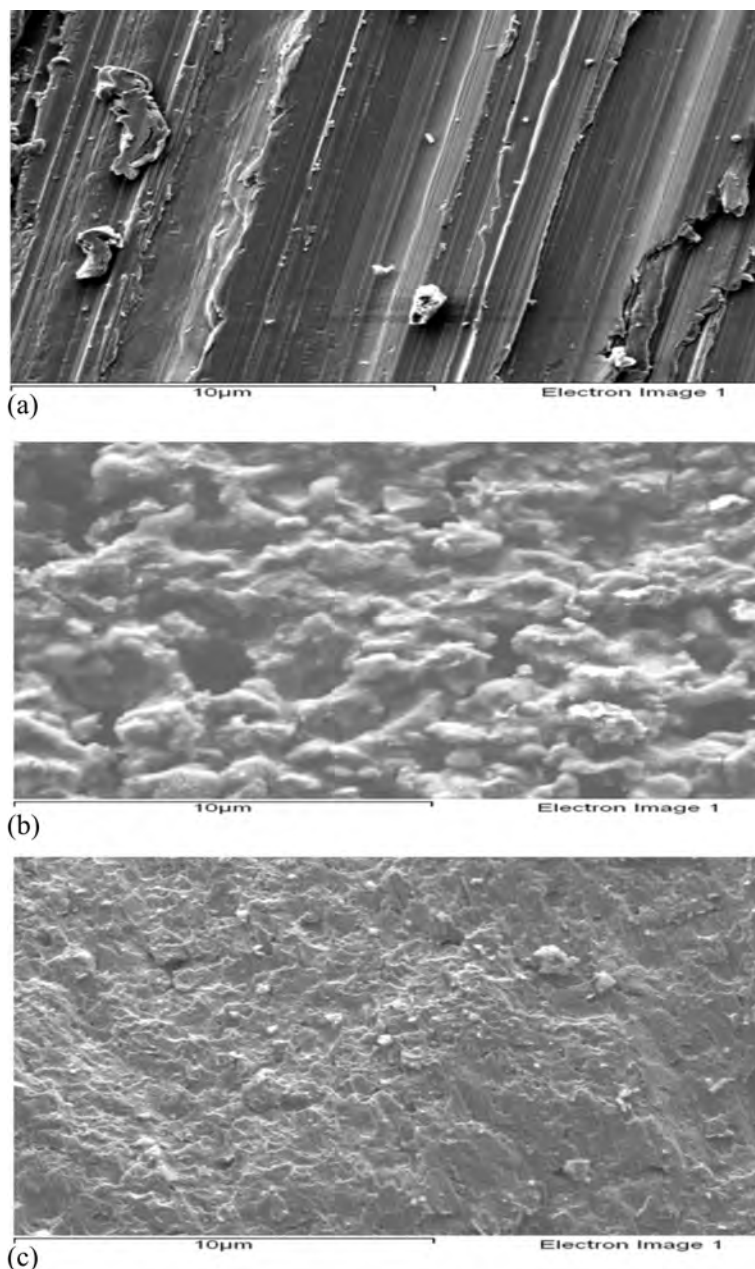
RESEARCH ARTICLE

R.T. Loto, C.A. Loto and A.P. Popoola,
S. Afr. J. Chem., 2015, **68**, 105–114,
<http://journals.sabinet.co.za/sajchem/>.

111

Figure 9 SEM micrographs of: (**a**) low carbon steel, (**b**) low carbon steel in 0.5 M H_2SO_4, and (**c**) low carbon steel in 0.5 M H_2SO_4 with MDMAE.

in Fig. 9c is significantly different from the control specimens in sulphuric acid. The amount of iron oxide formed and the inward protrusions are reduced as a result of the formation of a chemically adsorbed protective film of MDMAE on the steel. The adsorption of the negatively charged chloride and sulphate ions on the steel surface creates an excess negative charge leading to cation (protonated MDMAE) adsorption through electrostatic attraction onto the steel surface. The effective protection of the film is dependent on the concentration of MDMAE. Fig. 9c shows a specimen where the protective film of MDMAE adheres unto the steel even after removal from the test solution.

3.6. Adsorption Isotherms

The mechanism of corrosion inhibition can be explained on the basis of adsorption isotherms in order to understand the electrochemical interaction of the MDMAE adsorbate on the metal surface. Adsorptions isotherms help ascertain the intricacies of the physiochemical mechanism of inhibitor-metal relationship in acidic medium. The adsorption of corrosion inhibitors at the metal/solution interface is due to the formation of either electrostatic or covalent bonding between the adsorbate and the metal surface atoms. The Langmuir and Frumkin adsorption isotherms were applied to describe the adsorption mechanism for MDMAE in 0.5 M H_2SO_4. Both of these isotherms are of the general form:

$$f(\theta, x) \exp(-2a\theta) = KC \tag{8}$$

where $f(\theta, x)$ is the configurational factor which depends upon the physical model and assumptions underlying the derivative of the isotherm,[25] θ is the surface coverage, C is the inhibitor concentration, x is the size ratio, a is the molecular interaction parameter and K is the equilibrium constant of the adsorption process.

The Langmuir isotherm equation is expressed as shown in Equation 9:

$$\left[\frac{\theta}{1-\theta}\right] = K_{ads}C = K_{ads}C \tag{9}$$

and rearranging gives

RESEARCH ARTICLE

R.T. Loto, C.A. Loto and A.P. Popoola,
S. Afr. J. Chem., 2015, **68**, 105–114,
<http://journals.sabinet.co.za/sajchem/>.

112

$$\frac{c}{\theta} = \frac{1}{K_{ads}} C \tag{10}$$

where θ is the degree of coverage on the metal surface, C is the inhibitor concentration in the electrolyte, and K_{ads} is the equilibrium constant of the adsorption process. The plots of $\frac{c}{\theta}$ *versus* the inhibitor concentration C were linear (Fig. 10), indicating Langmuir adsorption.

The divergence of the slope from unity in Fig. 10 is due to the intermolecular relationship between the adsorbed inhibitor species on the metal surface and changes in the values of the Gibbs energy with increasing surface coverage. The Langmuir isotherm assumes all the adsorption sites are equivalent. The fitted line gave a value greater than unity for the slope. This suggests a slight deviation from ideal conditions assumed in the Langmuir model.

The Frumkin isotherm[26,27] assumes unit coverage at high inhibitor concentrations and that the electrode surface is inhomogeneous or that the lateral interaction effect is not negligible. In this way, only the active surface of the electrode, on which adsorption occurs, is taken into account.

The Frumkin adsorption isotherm can be expressed according to Equation 11:

$$\log\left\{C\left(\frac{\theta}{1-\theta}\right)\right\} = 2.303 \log K + 2\alpha\theta \tag{11}$$

where K is the adsorption-desorption constant and α is the lateral interaction term describing the interaction in the adsorbed layer.

Plots of $\theta/(1-\theta)$ *versus* inhibitor concentration (C) as presented in Fig. 11 are linear which shows the applicability of the Frumkin isotherm. The lateral interaction term (α) calculated from the slope of the Frumkin isotherm, indicates intermolecular repulsion between the inhibitor molecules on the surface of mild steel.[28] As surface coverage increases, lateral repulsion decreases, resulting in higher inhibition efficiency. Table 4 shows the relationship between the lateral interaction parameter and surface coverage (θ).

3.7. Thermodynamics of the Corrosion Process

The values of the Gibbs energy change (ΔG_{ads}) for the adsorption process is evaluated from the equilibrium constant of adsorption by means of Equation 12 and the data obtained are shown in Table 5.

$$\Delta G_{ads} = -2.303 \, RT\log [55.5K_{ads}] \tag{12}$$

where 55.5 is the molar concentration of water in the solution, R is the universal gas constant, T is the absolute temperature and K_{ads} is the equilibrium constant of adsorption. K_{ads} is related to surface coverage (θ) by the Langmuir relationship shown in Equation 9.

The results presented in Table 5 provide additional evidence of slight deviations from the ideal conditions of the Langmuir model as observed in the different values of the Gibbs energy of adsorption (ΔG_{ads}) with increase in surface coverage (θ). The dependence of the Gibbs energy of adsorption (ΔG_{ads}) of
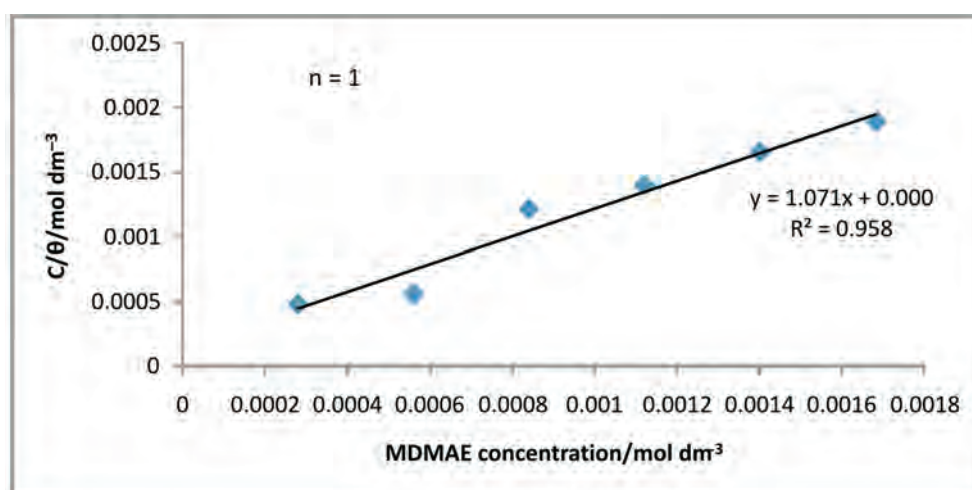

Figure 10 Langmuir adsorption isotherm plot of $\frac{C}{\theta}$ against inhibitor concentration in 0.5 M H_2SO_4
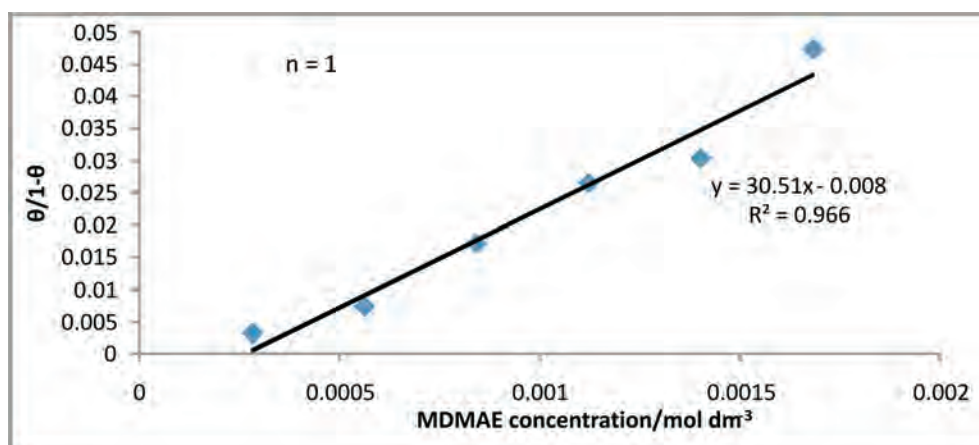

Figure 11 Frumkin isotherm relationship between ($\theta/1-\theta$) and inhibitor concentration (C) in 0.5 M H_2SO_4.

Table 4 Relationship between lateral interaction parameter, α, and surface coverage, θ ($n = 1$).

Lateral interaction	Surface coverage/θ
Parameter/α	
–0.0079	0.759
–0.0068	0.881
–0.0063	0.945
–0.0062	0.964
–0.0062	0.968
–0.0061	0.979

Table 5 Data obtained for the values of Gibbs energy, surface coverage and equilibrium constant of adsorption at varying concentrations of MDMAE in 0.5 M H_2SO_4 ($n=1$).

Samples	Surface coverage/θ	Equilibrium constant of adsorption/K_{ads}	Gibbs energy of adsorption (ΔG_{ads})/kJ mol^{-1}
A	0	0	0
B	0.759	11214.55	–33.03
C	0.881	13210.11	–33.49
D	0.945	20409.42	–34.52
E	0.964	23564.81	–34.92
F	0.968	21722.74	–34.69
G	0.979	28141.71	–35.32

MDMAE on surface coverage is ascribed to the heterogeneous nature of the steel. On low carbon steel not all sites can be equivalent on the surface due to heterogeneity, thus the different adsorption energies as observed in the experimental data (Table 5). The surface energy depends on the orientation of metal crystals and concentration of flaws (such as dislocations, vacancies, micro-distortions of the crystal lattice, etc.) at the interface.

Generally, values of ΔG_{ads} around –20 kJ mol^{-1} or below are consistent with electrostatic interaction between charged molecules and the charged metal (physisorption) those around –40 kJ mol^{-1} or higher involve charge sharing or transfer of electrons from the organic molecules to the metal surface to form a coordinate type of bond (chemisorption).[29,30] The value of ΔG_{ads} in H_2SO_4 depicts strong adsorption qualities. The negative values of ΔG_{ads} show that the adsorption of the inhibitor on the metal surface is spontaneous.[31] The average value of ΔG_{ads} for MDMAE is –34.33 kJ mol^{-1} indicating physiochemical interactions. Accordingly, the value of ΔG_{ads} obtained in the present study indicates that the adsorption mechanism of MDMAE on the steel is mainly chemisorption. The nitrogen and oxygen atoms of the inhibitor molecules are readily adsorbed onto the metal surface, forming insoluble stable films on the metal surface, thus decreasing metal dissolution. These cations of MDMAE are able to adsorb on the metal surface even at high concentration of anions of the acid. The anions (from the electrolyte) on the electrode surface provide strong electrostatic attraction, which promotes a direct adsorption of cations on the surface *via* formation of ion pairs. The strong attraction is responsible for the high values of the adsorption constant and the Gibbs energy of adsorption.

3.8. Statistical Analysis

A two-factor single level experimental ANOVA test (*F*-test)[13,14] was used to analyse the separate and combined effects of the percentage concentrations of MDMAE and exposure time on the inhibition efficiency of MDMAE in the corrosion of low carbon steels in 0.5 M H_2SO_4 solutions and to investigate the statistical significance of the effects. The *F*-test as shown in Table 6 was used to examine the amount of variation within each of the samples relative to the amount of variation between the samples.

The sum of squares among columns (exposure time) was obtained according to Equation 13:

$$SS_c = \frac{\sum T_c^2}{nr} - \frac{T^2}{N} \tag{13}$$

The sum of squares among rows (inhibitor concentration) was calculated according to Equation 14:

$$SS_r = \frac{\sum T_r^2}{nc} - \frac{T^2}{N} \tag{14}$$

The total sum of squares was obtained from Equation 15:

$$SS_{Total} = \sum x^2 - \frac{T^2}{N} \tag{15}$$

The results of the ANOVA test are tabulated in Table 6.

The analysis in 0.5 M H_2SO_4 was evaluated for a confidence level of 95 %, i.e. a significance level of $\alpha = 0.05$. The ANOVA results reveal the overwhelming influence of inhibitor concentration on the inhibition efficiency in comparison to the exposure time though both are statistically significant on the inhibition efficiency with *F*-values of 33.54 and 3.37. These are both greater than significance factor at $\alpha = 0.05$ (level of significance or probability). The statistical influence of the inhibitor concentration is 88.2 %, while the influence of the exposure time is 6.26 %. The inhibitor concentration and exposure time are significant model terms influencing inhibition efficiency of MDMAE on the corrosion of the steel specimen. The values show that inhibitor concentration plays a major role in the protection of the steel unlike some chemical compounds whose inhibition efficiency is strongly dependent on the length of time of exposure. This is a useful parameter for recommendation to government establishments and industrial firms. On this basis, the percentage concentration of MDMAE significantly affects the inhibition efficiency of MDMAE in the H_2SO_4 acid media.

4. Conclusions

Deanol showed excellent corrosion inhibition characteristics in the acidic medium; the corrosion rate reduced significantly with increase in concentration of deanol. The corrosion reaction

Table 6 Analysis of variance (ANOVA) for inhibition efficiency of MDMAE inhibitor in 0.5 M H_2SO_4 (at 95 % confidence level) ($n = 1$).

Source of variation	Sum of squares	Degrees of freedom	Mean square	Min. MSR at 95 % confidence		
				Mean square ratio	Significance *F*	*F*/%
Inhibitor concentration	1698.43	5	339.69	33.54	2.71	88.2
Exposure time	136.69	4	34.17	3.37	2.87	6.26
Residual	202.56	20	10.13			
Total	2037.68	29				

kinetics was significantly influenced by deanol thereby protecting the metal surface through adsorption which followed both the Langmuir and Frumkin adsorption isotherms. It showed cathodic inhibition properties at all concentrations from observation of the corrosion potential values of the polarization tests. At a confidence level of 95 %, the ANOVA results reveal only the inhibitor concentration to be statistically significant on the inhibition efficiency with a statistical influence of 88.5 %. SEM characterization shows surfaces to be topographically altered due to competitive adsorption of deanol onto the steel surface. The resulting topography consists of solid and impervious precipitates of deanol concentrates.

Acknowledgements

References

1 C.J. Philip, *Survey of Industrial Chemistry*, John Wiley & Sons, New York, USA, 1987, p. 45.

2 V.S. Sastri, *Corrosion Inhibitors Principles and Applications*, John Wiley & Sons, New York, 1998, p. 24.

3 S.S. Abd El-Rehim, M.A.M. Ibrahim and K.F. Khaled, 4-Aminoantipyrine as an inhibitor of mild steel corrosion in HCl solution, *J. Appl. Electrochem.*, 1999, **29**, 593–599.

4 J. Xu, L. Jiang and F. Xing, Influence of N, N'-dimethylaminoethanol as an inhibitor on the chloride threshold level for corrosion of steel reinforcement, *Mats. and Corr.*, 2010, **61**(9), 802–809.

5 G. Batis, E. Rakanta, B. Theodoridis, K.K. Sideris, K. Psomas and X. Barvari, Seventh CANMET/ACI International Conference on Superplasticizers and Other Chemical Admixtures in Concrete, 2003, 469–482.

6 E. Rakanta, E. Daflou and G. Batis, Evaluation of the monitoring of organic corrosion inhibition effectiveness, in *Measuring, Monitoring and Modelling Concrete Properties*, Springer, Netherlands, 2006, pp. 605–611.

7 I. Vyrides1, E. Rakanta, T. Zafeiropoulou and G. Batis, Efficiency of amino alcohols as corrosion inhibitors in reinforced concrete, *Open J. Civil Eng.*, 2013, **3**(2A), 1–8.

8 Dimethylethanolamine, http://en.wikipedia.org/wiki/Dimethylethanolamine, accessed 5 May 2014.

9 2-Dimethylaminoethanol, http://www.sigmaaldrich.com/catalog/product/aldrich/471453?Lang=en&region=NG [Accessed 5 May 2014].

10 N.C. Ngobiria, O. Akarantaa, N.C. Oforka, E.E. Oguzieb and S.U. Ogbuliec, Inhibition of pseudo-anaerobic corrosion of oil pipeline steel in pipeline water using biomas-derived molecules, *Advances Mats. Corros.*, 2013, **2**, 20–25.

11 G. Okamoto, M. Nagayama, J. Kato and T. Baba, Effect of organic inhibitors on the polarization characteristics of mild steel in acid solution, *Corros. Sci.*, 1962, **2**(1), 21–27.

12 P.M. Ejikeme, S. G. Umana, M.C. Menkiti and O.D. Onukwuli, Inhibition of mild steel and aluminium corrosion in 1 M H_2SO_4 by leaves extract of african breadfruit, *Int. J. Mats. Chem.*, 2015, **5**(1), 14–23.

13 A.S. Yaro, A.A. Khadom, R.K. Wael, Apricot juice as green corrosion inhibitor of mild steel in phosphoric acid, *Alexandria Eng. J.*, 2013, **52**(1), 129–135

14 P.J. Ramakrishnan, V.D. Janardhanan, R. Sreekumar and K.P. Mohan, Investigation on the effect of green inhibitors for corrosion protection of mild steel in 1 M NaOH solution, *Int. J. Corros.*, 2014. http://dx.doi.org/10.1155/2014/487103

15 A.A. Khedr, S.H. Sanad and K.M. El-Sobki, The influence of chloride ions in sulphuric acid on the corrosion behaviour of stainless steel, *Surf. Tech.*, 1984, **23**(2), 151–158

16 J. M. Gaidis, Chemistry of corrosion inhibitors, *Cement and Concrete Composites.*, 2004, **26**(3), 181–189

17 X. Wang, Y. Wan, Q. Wang, F. Shi, Z. Fan and Y. Chen, Synergistic inhibition between bisbenzimidazole derivative and chloride ion on mild steel in 0.25 M H_2SO_4 solution, *Int. J. Electrochem. Sci.*, 2013, **8**, 2182–2195.

18 M.R. Ali, C.M. Mustafa and M. Habib, Effect of molybdate, nitrite and zinc ions on the corrosion inhibition of mild steel in aqueous chloride media containing cupric ions, *J. Sci. Res.* 2009, **1**(1), 82–91.

19 X. Li, S. Deng, H. Fu and T. Li, Adsorption and inhibition effect of 6-benzylaminopurine on cold rolled steel in 1.0 M HCl, *Electrochim. Acta.*, 2009, **54**(16), 4089–4098.

20 Q. Qu, Z. Hao, S. Jiang, L. Li and W. Bai, Synergistic inhibition between dodecylamine and potassium iodide on the corrosion of cold rolled steel in 0.1 M phosphoric acid, *Mats. & Corr.*, 2008, **59**(11), 883–888.

21 F. Bentiss, M. Traisnel and M. Lagrenee, The substituted 1, 3, 4-oxadiazoles: a new class of corrosion inhibitors of mild steel in acidic media, *Corros. Sci.*, 2000, **42**(1), 127–146.

22 E.E. Oguzie, V.O. Njoku, C.K. Enenebeak, C.O. Akalezi and C.Obi, Effect of hexamethylpararosaniline chloride (crystal violet) on mild steel corrosion in acidic media, *Corros. Sci.*, 2008, **50**(12), 3480–3486.

23 L.Cáceresa, T. Vargasb and L. Herrerab, Influence of pitting and iron oxide formation during corrosion of carbon steel in unbuffered NaCl solutions, *Corros. Sci.*, 2009, **51**(5), 971–978.

24 Y.F. Chenga, M. Wilmottb and J.L. Luoa, The role of chloride ions in pitting of carbon steel studied by the statistical analysis of electrochemical noise, *App. Surf. Sci.*, 1999, **152**(3-4), 161–168.

25 M. Karakus, M. Sahin and S. Bilgic, An investigation on the inhibition effects of some new dithiophosphonic acid monoesters on the corrosion of the steel in 1 M HCl medium, *Mater. Chem. Phys.*, 2005, **92**, 565–571.

26 S. Paul and B. Kar, Mitigation of mild steel corrosion in acid by green inhibitors: yeast, pepper, garlic, and coffee, *ISRN Corrosion.*, 2012, http://dx.doi.org/10.5402/2012/641386

27 J.T. Nwabanne and V.N. Okafor, Inhibition of the corrosion of mild steel in acidic medium by Vernonia amygdalina: adsorption and thermodynamics study, *J. Emerg. Trends Eng. Appl. Sci.*, 2011, **2**, 619–625.

28 I.S. Martinez, Thermodynamic characterization of metal dissolution and inhibitor adsorption processes in the low carbon steel/mimosa tannin/sulfuric acid system, *Appl. Surf. Sci.*, 2002, **199**(1-4), 83–89.

29 I.B. Obot, N.O. Obi-Egbedi and S.A. Umoren, Experimental and theoretical investigation of clotrimazole as corrosion inhibitor for aluminium in hydrochloric acid and effect of iodide ion addition, *Der Pharma Chemica*, 2009, **1**(1), 151–166.

30 M.G. Hosseini, S.F.L. Mertens and M.R. Arshadi, Synergism and antagonism in mild steel corrosion inhibition by sodium dodecylbenzenesulphonate and hexamethylenetetramine, *Corros. Sci.*, 2003, **45**(7), 1473–1489.

31 B. Obot, N.O. Obi-Egbedi and S.A. Umoren, Experimental and theoretical investigation of clotrimazole as corrosion inhibitor for aluminium in hydrochloric acid and effect of iodide ion addition, *Der. Pharm. Chem.*, 2009, **1**, 151–166